Material and Methods

Clinical samples

Ninety-three CRC patients underwent surgical treatment at the Kyushu University at Beppu and affiliated hospitals between 1993 and 1999. Resected tumor and paired nontumor tissue specimens were immediately cut from resected colon and placed in RNAlater (Takara, Japan) or embedded in Tissue Tek OCT medium (Sakura, Tokyo, Japan), or frozen in liquid nitrogen and kept at −80°C until RNA extraction. Written informed consent was obtained from all patients. The median follow-up period was 3.0 years.

Quantitative RT-PCR

The sequences of *FBXW7* mRNA primers were as follows: sense, 5′-AAA GAG TTG TTA GCG GTT CTC G-3′; antisense, 5′-CCA CAT GGA TAC CAT CAA ACT G-3′. Glyceraldehyde-3-phosphate dehydrogenase (*GAPDH*) was used as an internal control and *GAPDH* primers were as follows: sense, 5′-TTG GTA TCG TGG AAG GAC TCT A-3′; antisense, 5′-TGT CAT ATT TGG CAG GTT-3′. Real-time monitoring of PCR reactions was performed using the LightCycler™ system (Roche Applied Science, Indianapolis, IN) and SYBER-Green I dye (Roche Applied Science, Indianapolis, IN). Monitoring was performed according to the manufacturer's instructions, as described previously.[8] In brief, a master mixture was prepared on ice, containing 1 μL of cDNA, 2 μL of DNA Master SYBER-Green I mix, 50 ng of primers and 2.4 μL of 25 mM $MgCl_2$. The final volume was adjusted to 20 μL with water. After the reaction mixture was loaded into glass capillary tubes, quantitative RT-PCR was performed with the following cycling conditions: initial denaturation at 95°C for 10 min, followed by 40 cycles of 95°C for 10 sec, annealing at 62°C for 10 sec and extension at 72°C for 10 sec. After amplification, products were subjected to a temperature gradient from 67°C to 95°C at 0.2°C/sec, under continuous fluorescence monitoring, to produce a melting curve of products.

Data analysis for Quantitative RT-PCR

We used the LightCycler® Software version 3.5 program (Roche Molecular Biochemicals) to calculate the cycle numbers. After proportional baseline adjustment, the fit point method was employed to determine the cycle in which the log-linear signal was first distinguishable from the baseline. This cycle number was used as the crossing point value. A standard curve was produced by measuring the crossing point of each standard value and plotting it against the logarithmic concentration value. Concentrations of unknown samples were calculated by plotting their crossing points against the standard curve and dividing by *GAPDH* content. *GAPDH* expression levels were the same in tumor and normal tissues.

Immunohistochemistry

Immunohistochemical studies for FBXW7, c-Myc and cyclin E were performed on formalin-fixed, paraffin-embedded surgical sections obtained from 71 patients with CRC. Tissue sections were deparaffinized, soaked in 0.01 M sodium citrate buffer and boiled in a microwave for 5 min at 500 W to retrieve cell antigens. The primary mouse monoclonal antibodies against FBXW7 (Abnova Corporation, Taipei, Taiwan), mouse monoclonal antibodies against c-Myc (sc-40, Santa Cruz Biotechnology, CA) and rabbit polyclonal antibodies against Cyclin E (SC-481, Santa Cruz Biotechnology) were used at dilutions of 1:100, 1:50 and 1:50, respectively. Tissue sections were immunohistochemically stained using ENVISION reagents (ENVISION+ Dual Link System-HRP, Dako Cytomation, Glostrup, Denmark). All sections were counterstained with hematoxylin. We confirmed the specificity of antibody for *FBXW7* using by the thymus of *Fbxw7* knockout mouse established by Onoyama *et al.*[7] (Supporting Information, Fig. 4).

Laser microdissection

The tissues from another series of 130 patients with CRC were collected for laser micro-dissection (LMD). CRC tissues were microdissected using the LMD system (Leica Laser Microdissection System, Leica Microsystems, Wetzlar, Germany) as previously described.[9] For LMD, 5 μ frozen sections were fixed in 70% ethanol for 30 sec, stained with hematoxylin and eosin and dehydrated as follows: 5 sec each in 70%, 95% and 100% ethanol and a final 5 min in xylene. Sections were air-dried, then microdissected with the LMD system. Target cells were excised, at least 100 cells per section, and bound to the transfer film, and total DNA extracted.

cDNA-microarray

We used the commercially available Human Whole Genome Oligo DNA Microarray Kit (Agilent Technologies, Santa Clara, CA). A list of genes on this cDNA microarray is available from http://www.chem.agilent.com/scripts/generic.asp?lpage=5175 &indcol=Y&prodcol=Y&prodcol=N&indcol=Y&prodcol=N. Cyanine (Cy)-labeled cRNA was prepared using T7 linear amplification as described in the Agilent Low RNA Input Fluorescent Linear Amplification Kit Manual (Agilent Technologies). Labeled cRNA was fragmented and hybridized to an oligonucleotide microarray (Whole Human Genome 4 × 44K Agilent G4112F). Fluorescence intensities were determined with an Agilent DNA Microarray Scanner and were analyzed using G2567AA Feature Extraction Software Version A.7.5.1 (Agilent Technologies), which used the LOWESS (locally weighted linear regression curve fit) normalization method.[10] This microarray study followed MIAME guidelines issued by the Microarray Gene Expression Data group.[11] Further analyses were performed using GeneSpring version 7.3 (Silicon Genetics, San Carlos, CA).

Array-CGH

Array-CGH was performed using the Agilent Human Genome Microarray Kit 244K (Agilent Technologies). The array-CGH platform is a high resolution 60-mer oligonucleotides based

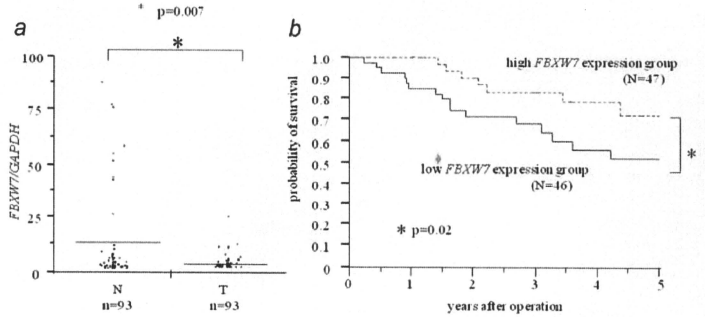

Figure 1. Clinical significance of *FBXW7* mRNA expression in CRC. (*a*) *FBXW7* mRNA expression in cancerous and normal tissues from CRC patients as assessed by real-time quantitative PCR ($n = 93$). Horizontal lines indicate mean value of each group (T, cancer tissue; N, noncancerous tissue). (*b*) Kaplan-Meier five year overall survival curves for CRC patients according to the level of *FBXW7* mRNA expression. The overall survival rate for patients in the high expression group was significantly higher than that for patients in the low expression group ($p = 0.02$). High expression group (broken line: $N = 47$), low expression group (unbroken line: $N = 46$).

microarray containing about 244,400 probes spanning coding and non-coding genomic sequences with median spacing of 7.4 kb and 16.5 kb, respectively. Labeling and hybridization were performed according to the protocol provided by Agilent (Protocol v4.0, June 2006). Arrays were analyzed using The Agilent DNA microarray scanner.

Array-CGH data analysis

The raw signal intensities of tumor DNAs were measured with Human Genome CGH Microarray 244K (Agilent Technologies) which were then transformed into log ratio to reference DNA with 'Feature Extraction' software (v9.1) of Agilent Technologies. The log ratio was thereafter used as the signal intensity of each probe. One hundred thirty samples from different patients were subjected to circular binary segmentation (CBS) after median normalization.[12] An R script written by us was used for the median normalization, whereas an R program implemented in the "DNA copy" package of the Bioconductor project (http://www.bioconductor.org) was used for the CBS analysis. Instead of all of the CGH probes, 13,403 probes from chromosome 4 (NCBI Build 35) were analyzed in this study. An absolute log2 ratio >0.263 was used as the threshold for the gain or loss in DNA copy number for each probe.

Total RNA extraction and first-strand cDNA synthesis

Frozen tissue specimens or cultured cell lines at subconfluency were homogenized, and total RNA was extracted using the modified acid-guanidine-phenol-chloroform method as described previously.[13,14] Total RNA (8.0 μg) was reverse transcribed to cDNA using M-MLV RT (Invitrogen Corp. Carlsbad, CA).

Cell lines

The human CRC cell lines, LoVo and Colo 201, were obtained from the Japanese Collection of Research Bioresoureces (JCRB, Osaka, Japan). The cell lines were maintained in Ham's F-12 medium and RPMI1640 (Invitrogen Corp.) supplemented with 10% fetal bovine serum (Equitech-Bio, Kerrville, TX), 100 units/mL penicillin G and streptomycin (Invitrogen Corp.). The cells were incubated in 5% CO_2 at 37°C and passaged every three days.

FBXW7 RNA interference

FBXW7-specific siRNA (Silencer™ Predesigned siRNA) was purchased from Ambion, USA. siRNA oligomer was diluted with Opti-MEM I® Medium without serum (Invitrogen Corp.). The diluted siRNA oligomer was mixed with the diluted Lipofectamine™ RNAiMAX (Invitrogen Corp.) and incubated for 15 min at room temperature to allow siRNA-Lipofectamine™RNAiMAX complexes to form. Diluted logarithmic growth-phase LoVo cells without antibiotics were seeded at 2×10^5 cells/well in a final volume of 2 mL or 100 μL in 6 or 96 well flat bottom microtiter plates, respectively. The cells were incubated in a humidified atmosphere (37°C and 5% CO_2). The assay was performed after 72 hr incubation.

Table 1. *FBXW7* mRNA expression and clinocopathological factors

Factors	High expression (n = 47)		Low expression (n = 46)		p value
	n	%	n	%	
Age (mean ± SD)	67.4 ± 10.0		67.4 ± 11.6		0.98
Sex					0.07
Male	30	63.8	22	47.8	
Female	17	36.2	24	52.2	
Histological grade					0.42
Well	19	40.4	14	30.4	
Moderately, poorly others	28	59.6	32	69.6	
Size					0.32
>30 mm (small)	10	21.3	11	23.9	
<31 mm (large)	37	78.7	35	76.1	
Depth of tumor invasion[1]					0.03
m, sm, sp	36	78.3	27	57.5	
s, se, si	10	22.7	20	42.5	
Lymph node metastasis					0.76
Absent	21	44.7	20	43.5	
Present	26	55.3	26	56.5	
Lymphtic invasion					0.59
Absent	29	61.7	25	54.3	
Present	18	38.3	21	45.7	
Venous invasion					0.23
Absent	43	91.5	38	82.6	
Present	4	8.5	8	17.4	
Liver metastasis					0.48
Absent	44	93.6	41	89.1	
Present	3	6.4	5	10.9	
Peritoneal dissemination					0.24
Absent	47	100.0	45	97.8	
Present	0	0.0	1	2.2	
Duke's stage					0.47
A, B	23	50.0	27	57.5	
C, D	3	50.0	20	42.5	

[1]Tumor invasion of mucosa (m), submucosa (sm), muscularis propria (mp), subserosa (ss), penetration of serosa (se), and invasion.

Western blot analysis

Total protein was extracted from cell lines using protein extraction solution (PRO-PREP, iNtRON Biotechnology, Korea). Total protein (40 μg) was electrophoresed in 10% concentrated READY GELS J (Bio-Rad Laboratories, Japan) and electroblotted onto pure nitrocellulose membranes (Trans-Blot Transfer Medium; Bio-Rad Laboratories, Japan) at 0.2 A for 120 min. c-Myc protein was detected using mouse monoclonal antibodies (sc-40, Santa Cruz Biotechnology) diluted 1:500. Cyclin E protein was detected using rabbit polyclonal antibodies (SC-481, Santa Cruz Biotechnology) diluted 1:100. c-Myc and cyclin E protein levels were normalized to the level of β-actin protein (Cytoskeleton, Denver CO) diluted 1:1,000. Blots were developed with horse-radish peroxidase-linked anti-mouse and rabbit immunoglobulin (Promega, Madison, WI) diluted 1:1,000. ECL Detection Reagents (Amersham Biosciences, Piscataway, NJ) were used to detect antigen-antibody reactions.

Proliferation assay

Proliferation of the cell lines was determined by 3-(4, 5-dimethylthiazol-2-yl)-2, 5-diphenyl tetrazolium bromide (MTT)

Table 2. Univariate and multivariate analysis for overall survival (Cox proportional regression model)

	Univariate analysis			Multivariate analysis		
Factors	**RR**	**95% CI**	***p* value**	**RR**	**95% CI**	***p* value**
Age (<65/<66)	0.820	0.540–1.218	0.328	–	–	–
Sex (male/female)	0.822	0.538–1.228	0.342	–	–	–
Histology grade (well/moderately and poorly & others)	0.690	0.416–1.063	0.095	–	–	–
Tumor size (<30 mm/>31 mm)	1.285	0.792–2.380	0.331	–	–	–
Depth of tumor invasion[1] (m, sm, mp/ss, se, si)	1.738	1.101–3.024	0.016	1.78	1.075–3.095	0.023
Lymph node metastasis(negative/positive)	2.014	1.329–3.231	0.001	2.145	1.368–3.563	0.001
Lymphatic invasion (negative/positive)	2.326	1.529–3.744	0.001	–	–	–
Venous invasion (negative/positive)	1.852	1.145–2.845	0.014	1.825	1.106–2.891	0.020
FBXW7 mRNA expression (low/high)	1.564	1.027–2.516	0.036	1.983	1.264–3.267	0.003

[1]Tumor invasion of mucosa (m), submucosa (sm), muscularis propria (mp), subserosa (ss), penetration of serosa (se), and invasion of adjacent strucures (si). Abbreviations: RR, relative risk; CI, confidence interval.

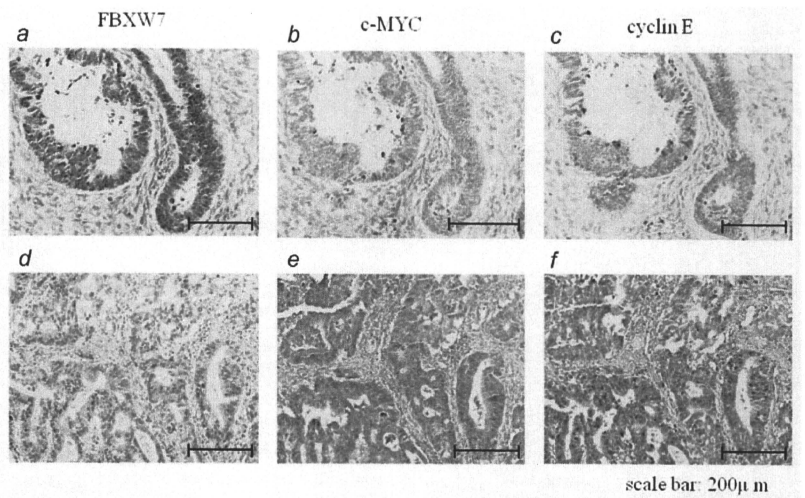

Figure 2. Immunohistochemical analysis of FBXW7, c-MYC and cyclin E expression in CRC. In cases of high FBXW7 protein expression (*a*), there was no detectable c-MYC (*b*) or cyclin E (*c*) protein expression in the same tissue section. In contrast, in the case of low FBXW7 protein expression (*d*), there was strong c-MYC (*e*) and cyclin E (*f*) protein expression (×200 original magnification). [Color figure can be viewed in the online issue, which is available at www.interscience.wiley.com.]

assay (Roche Diagnostics GmbH, Mannheim, Germany). After 24 hr incubation with siRNA, cells were seeded at 5×10^3 cells well^{-1} in microtiter plates (96 wells, flat bottom) in a final volume of 100 μL culture medium per well, in a humidified atmosphere (37°C and 5% CO_2). After 72 hr incubation, 10 μL of MTT labeling agent (final concentration 0.5 mg mL^{-1}) was added to each well. The microtiter plate was incubated for 4 hr in a humidified atmosphere. Solubilization solution (100 μL) was added to each well. The plate was allowed to stand overnight in the incubator in a

humidified atmosphere. After checking for complete solubilization of the purple formazan crystals, spectrophotometric absorbance of the sample was measured using a model 550 microplate reader (Bio-Rad Laboratories, CA), at a wavelength of 570 nm corrected 655 nm. Each independent experiment was performed three times.

Statistical analysis

For continuous variables, data were expressed as the mean ± standard deviation. The relationship between *FBXW7* mRNA expression and clinicopathological factors was analyzed using a χ^2 test and Student's *t*-test. Overall survival curves were plotted according to the Kaplan-Meier method and the generalized Log-rank test was applied to compare the survival curves. All tests were analyzed using JMP software (SAS Institute Inc., Cary, NC) and the findings were considered significant for p values <0.05.

Results

Expression of FBXW7 mRNA in clinical tissue specimens

FBXW7 mRNA expression was examined in 93 CRC clinical samples using reverse transcription-polymerase chain reaction (RT-PCR) and real-time quantitative RT-PCR, with quantified values used to calculate *FBXW7*/*GAPDH* ratios. In these samples, clinicopathological factors, including prognosis, were available. The mean expression level of *FBXW7* mRNA in tumor tissue specimens was significantly lower than that of nontumor tissue ($p = 0.007$) (Fig. 1*a*).

FBXW7 mRNA expression and clinicopathological characteristics

We divided the 93 CRC cases into two groups according to the median tumor (*T*)/normal (*N*) ratio of *FBXW7* mRNA expression level as determined above. Thus, 46 cases were placed in the high *FBXW7* expression group and 47 cases in the low *FBXW7* expression group. The association between clinicopathological features and *FBXW7* mRNA expression is summarized in Table 1. In the low *FBXW7* expression group, tumor invasion was significantly elevated compared to the high *FBXW7* expression group ($p = 0.02$). Univariate analysis identified *FBXW7* expression, tumor invasion, lymph node metastasis, lymphatic invasion and venous invasion as prognostic factors for 5-year overall survival following surgery. Variables with p values <0.05 by univariate analysis were selected for multivariate analysis using Cox's proportional hazards model. *FBXW7* expression [relative risk (RR): 1.98, confidence interval (CI): 1.26–3.26, $p = 0.003$] was found to be a significant factor affecting five year overall survival following surgery (Table 2). Analysis of 5-year overall survival curves showed that patients in the low *FBXW7* expression group had a significantly poorer prognosis than those in the high expression group ($p = 0.02$) (Fig. 1*b*).

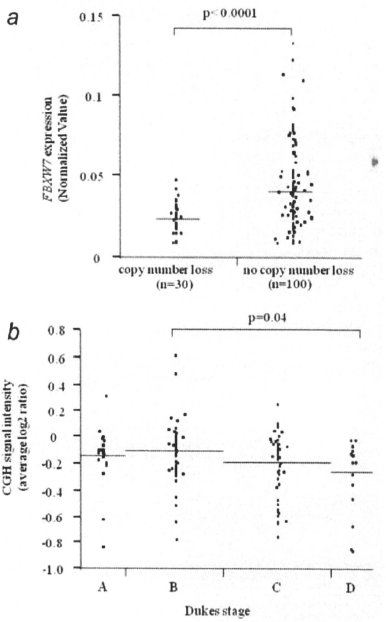

Figure 3. Concordant loss of *FBXW7* expression and copy number alteration in the flanking region of *FBXW7*. There were 30 cases with deletions and 100 cases without loss in CRC. The expression of *FBXW7* in the deleted cases was significantly lower than the cases with wild type *FBXW7* ($p < 0.0001$). (*a*) CGH signal intensity (average log2 ratio) according to Dukes staging classification. (*b*) The ratio of copy number loss of *FBXW7* increased along with the progression of Dukes' stage.

Immunohistochemical determination of FBXW7, c-MYC and cyclin E expression

Expression of FBXW7 protein was evaluated by immunohistochemistry of resected CRC specimens, using an anti-FBXW7 antibody. When FBXW7 protein was expressed at high levels, expression of c-MYC and cyclin E protein was below detection (Figs. 2*a–c*). This patient had a 5-year, recurrence-free survival after curative surgery despite the advanced stage. In contrast, in cases of low FBXW7 protein expression, strong expression of c-MYC and cyclin E proteins was noted (Figs. 2*d–f*). This patient died from peritoneal dissemination six months after curative surgery. We examined the association between *FBXW7* and *c-MYC* or *Cyclin E* in serial

Table 3. The copy number loss of *FBXW7* and clinocopathological factors

Factors	Copy number loss group (n = 30)		No abberant group (n = 100)		p value
	n	%	n	%	
Age (mean ± SD)	67.4 ± 10.0		67.4 ± 10.0		0.293
Sex					0.107
Male	13	43.3	60	60.0	
Female	17	56.7	40	40.0	
Histological grade					0.439
Well	15	50.0	58	58.0	
Moderately, poorly others	15	50.0	42	42.0	
Size					0.157
>30 mm (small)	8	26.7	15	15.0	
<31 mm (large)	22	76.3	85	85.0	
Depth of tumor invasion[1]					1.000
m, sm, sp	24	80.0	80	80.0	
s, se, si	6	20.0	20	20.0	
Lymph node metastasis					0.049
Absent	11	36.7	57	57.0	
Present	19	63.3	43	43.0	
Lymphtic invasion					0.021
Absent	8	26.7	50	50.0	
Present	22	73.3	50	50.0	
Venous invasion					0.049
Absent	7	2.3.3	42	42.0	
Present	23	76.7	58	58.0	
Liver metastasis					0.098
Absent	24	80.0	91	91.0	
Present	6	20.0	9	9.0	
Peritoneal dissemination					0.683
Absent	29	96.7	98	98.0	
Present	1	3.3	2	2.0	
Duke's stage					0.045
A, B	10	33.3	54	54.0	
C, D	20	66.7	46	46.0	

[1]Tumor invasion of mucosa (m), submucosa (sm), muscularis propria (mp), subserosa (ss), penetration of serosa (se), and invasion of adjacent strucures (si).

sections of 71 cases by immunohistochemical study. Seventy one CRC samples were divided into three groups according to *FBXW7* protein level (high = 16, medium = 19 and low = 36). We compared the expression between *FBXW7* protein and mRNA in 52 cases with high and low *FBXW7* protein level. The expression level of *FBXW7* mRNA in high *FBXW7* protein group (n = 16) is significantly higher than that in low *FBXW7* protein group (n=36) (Supporting Information 3*a*, p = 0.03). Furthermore, we found the significant inverse correlation between *FBXW7* and *c-MYC* or *cyclin E*. (supporting information, Fig. 3*b*: *FBXW vs. c-MYC*: $r = -0.526$, $p < 0.0001$, *FBXW7 vs. cyclin E*: $r = -0.553$, $p < 0.0001$).

Aberrations in FBXW7 copy number in CRC specimens

To clarify the cause of suppression of *FBXW7* mRNA in patients with poorer prognosis, we investigated copy number aberrations of *FBXW7* in 130 CRC specimens using laser micro-dissection and CGH array. As shown in Figure 3*a*, there was a significant correlation between expression of *FBXW7* and copy number of the *FBXW7* region (Fig. 3*a*) ($p < 0.0001$). Therefore, loss of *FBXW7* expression described

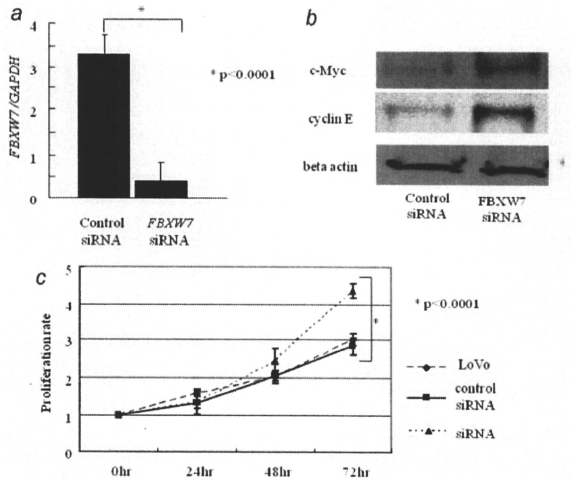

Figure 4. Effect of *FBXW7* gene silencing on a colon cancer cell line. (*a*) *FBXW7* mRNA in LoVo cells was suppressed by *FBXW7* siRNA as confirmed by quantitative RT-PCR. (*b*) Expression of c-MYC and cyclin E proteins was enhanced by *FBXW7* siRNA, as confirmed by Western blot analysis. These proteins were normalized to the level of beta actin. (*c*) The proliferation rate of LoVo cells treated with *FBXW7* siRNA (dotted line) was significantly greater than that in control siRNA cells (unbroken line) and parent LoVo cells (broken line).

above was caused by genetic alteration in the flanking region of *FBXW7*. Figure 3*b* shows CGH signal intensity (average log2 ratio) according to Dukes staging classification (Supporting Information, Fig. 1: heat map representation of copy number aberration of *FBXW7* according to Dukes staging classification). Thirty cases (23.1%) had at least one copy number aberration in all cases. The ratio of copy number loss of *FBXW7* increased along with the progression of Dukes' stage. The association between clinicopathological features and the copy number of *FBXW7* is summarized in Table 3. In the copy number loss group, lymphatic invasion, venous invasion and lymph node metastasis was increased compared with the nonaberrant group (Table 3, $p = 0.02$, $p = 0.04$ and $p = 0.04$, respectively). In addition, the copy number loss group had more advanced cases compared with the nonaberrant group ($p = 0.04$).

Effect of FBXW7 gene silencing on CRC cell lines

LoVo cells expressed *FBXW7* mRNA at a high level as confirmed by RT-PCR. We examined whether suppression of *FBXW7* would enhanced c-Myc and cyclin E protein expression, both of which are degradation targets of *FBXW7*. The expression level of *FBXW7* mRNA was suppressed by *FBXW7*-specific siRNA as confirmed by RT-PCR analysis (Fig. 4*a*). We found that the protein expression levels of c-Myc and cyclin E were enhanced by *FBXW7*-specific siRNA as confirmed by Western blotting analysis (Fig. 4*b*). Furthermore, we evaluated the proliferation activity of LoVo cells suppressed by *FBXW7*-specific siRNA using MTT assays. We found that the proliferation rate in LoVo cells suppressed by *FBXW7* siRNA significantly increased compared to that in control cells (Fig. 4*c*). We demonstrated that similar phenomena are found in Colo 201 (Supporting Information, Fig. 5).

Discussion

In our current study, we found that *FBXW7* mRNA gene expression was significantly suppressed in human CRC tissue compared to the corresponding normal tissue ($p = 0.007$) and that the patients in the low *FBXW7* expression group had a significantly poorer prognosis than those in the high expression group ($p = 0.02$). We also examined how loss of *FBXW7* contributed to cell growth.

We found that approximately 25% of patients with CRC have a reduced copy number of *FBXW7*, and that the incidence of genetic alteration was concordantly increased with the progression of disease stage. Tsafrif *et al.* and Lassmann *et al.* previously reported that particular chromosomal

regions and genes that are frequently gained and overexpressed (e.g., 7p, 8q, 13q and 20q) or lost and underexpressed (e.g., 1p, 4, 5q, 8p, 14q, 15q and 18).[15,16] Our current array-CGH data is consistent with their previous data (Supporting Information, Fig. 2). Chromosome 4q, containing the *FBXW7* gene, is deleted in various carcinomas such as esophageal, gastric, and breast cancer.[17,18] Rajagopalan *et al.* previously reported that the deficiency of *FBXW7* in CRC is associated with genetic instability.[19] The mutations in *FBXW7* in colorectal tumor have been found in 6–8%.[19,20] However, Kemp *et al.* suggested that mutations in *FBXW7* in colorectal tumor do not affect the chromosomal instability and result in biallelic inactivation.[20] We found that *FBXW7* was altered at the genetic level in CRC as determined by LMD and CGH array. Our findings that *FBXW7* gene copy number loss frequently occurred in CRC may provide insight into how *FBXW7* function is inactivated during cancer development.

The decrease of FBXW7 expression gave rise to abnormal accumulation of c-MYC and cyclin E protein.[21] MYC protein plays crucial roles in mitogenic and cell growth responses and is commonly deregulated in cancers.[22] Cyclin E is a key component of the cell cycle machinery that is frequently deregulated in cancer.[23] Our current study indicated that FBXW7 regulates c-MYC and cyclin E *in vitro*. In fact, it appears that FBXW7 normally inhibits c-Myc and cyclin E and thereby promotes exit from the cell cycle at G1-S phase. Those findings suggest that *FBXW7* may be a tumor suppressor gene and loss of the gene could prevent cells from entering a quiescent state. Thus, it is possible that introduction of *FBWX7* gene or protein could force tumors into dormancy.

According to Figure 3*a*, all CRC cases with genetic alterations exhibited diminished *FBXW7* expression. However, 65 cases (65%) in Figure 3*a* showed loss of *FBXW7* expression without genetic alteration. To explain this finding, we speculate theremay be epigenetic transcriptional regulation,[24] translational regulation by non-coding RNA or upregulation of Wnt/beta-catenin signals from interstitial niche cells associated with cancer cells.

In conclusion, multivariate analysis showed that *FBXW7* expression in CRC is an independent prognostic factor for five year survival following surgery. *FBXW7* may be useful as a prognostic indicator in CRC. Cell cycle regulation by ubiquitin ligase has potential in developing new targets in cancer therapy.

Acknowledgements

We thank Ms. T. Shimooka, Mrs. K. Ogata, Ms. M. Kasagi, Ms. Y. Nakagawa and Ms. T. Kawano for their technical assistance. The novelty and impact of this article is that we firstly investigated the copy number aberrations of FBXW7 in a series of 130 human colorectal cancer (CRC) specimens with laser microdissection by comprehensive genome hybridization (CGH) array and FBXW7 gene expression in another subset of 93 CRC samples with clinicopathlogic factors, including prognosis. Furthermore, those identified findings of the clinicopathologic significance of FBXW7 repression was validated biologically by CRC cell line with siRNA interference, which showed FBXW7 repression accelerated the cell cycle to determine a prognostic factor in CRC cases.

References

1. Bashir T, Pagano M. Aberrant ubiquitin-mediated proteolysis of cell cycle regulatory proteins and oncogenesis. *Adv Cancer Res* 2003;88:101–44.
2. Akhoondi S, Sun D, von der Lehr N, Apostolidou S, Klotz K, Maljukova A, Cepeda D, Fiegl H, Dafou D, Marth C, Mueller-Holzner E, Corcoran M, et al. FBXW7/hCDC4 is a general tumor suppressor in human cancer. *Cancer Res* 2007;67:9006–12.
3. Mao JH, Perez-Losada J, Wu D, Delrosario R, Tsunematsu R, Nakayama KI, Brown K, Bryson S, Balmain A. Fbxw7/Cdc4 is a p53-dependent, haploinsufficient tumour suppressor gene. *Nature* 2004;432:775–9.
4. Welcker M, Clurman BE. FBW7 ubiquitin ligase: a tumour suppressor at the crossroads of cell division, growth and differentiation. *Nat Rev Cancer* 2008;8:83–93.
5. Sonoda H, Inoue H, Ogawa K, Utsunomiya T, Masuda TA, Mori M. Significance of skp2 expression in primary breast cancer. *Clin Cancer Res* 2006;12:1215–20.
6. Nakayama KI, Nakayama K. Ubiquitin ligases: cell-cycle control and cancer. *Nat Rev Cancer* 2006;6:369–81.
7. Onoyama I, Tsunematsu R, Matsumoto A, Kimura T, de Alboran IM, Nakayama K, Nakayama KI. Conditional inactivation of Fbxw7 impairs cell-cycle exit during T cell differentiation and results in lymphomatogenesis. *J Exp Med* 2007;204:2875–88.
8. Ogawa K, Utsunomiya T, Mimori K, Tanaka F, Inoue H, Nagahara H, Murayama S, Mori M. Clinical significance of human kallikrein gene 6 messenger RNA expression in colorectal cancer. *Clin Cancer Res* 2005;11:2889–93.
9. Nishida K, Mine S, Utsunomiya T, Inoue H, Okamoto M, Udagawa H, Hanai T, Mori M. Global analysis of altered gene expressions during the process of esophageal squamous cell carcinogenesis in the rat: a study combined with a laser microdissection and a cDNA microarray. *Cancer Res* 2005;65:401–9.
10. Quackenbush J. Microarray data normalization and transformation. *Nat Genet* 2002;32 (Suppl):496–501.
11. Brazma A, Hingamp P, Quackenbush J, Sherlock G, Spellman P, Stoeckert C, Aach J, Ansorge W, Ball CA, Causton HC, Gaasterland T, Glenisson P, et al. Minimum information about a microarray experiment (MIAME)-toward standards for microarray data. *Nat Genet* 2001;29:365–71.
12. Venkatraman ES, Olshen AB. A faster circular binary segmentation algorithm for the analysis of array CGH data. *Bioinformatics* 2007;23:657–63.
13. Utsunomiya T, Hara Y, Kataoka A, Morita M, Arakawa H, Mori M, Nishimura S. Cystatin-like metastasis-associated protein mRNA expression in human colorectal cancer is associated with both liver metastasis and patient survival. *Clin Cancer Res* 2002;8:2591–4.
14. Utsunomiya T, Okamoto M, Hashimoto M, Yoshinaga K, Shiraishi T, Tanaka F, Mimori K, Inoue H, Watanabe G, Barnard GF, Mori M. A gene-expression signature can quantify the degree of hepatic fibrosis in the rat. *J Hepatol* 2004;41:399–406.
15. Lassmann S, Weis R, Makowiec F, Roth J, Danciu M, Hopt U, Werner M. Array CGH identifies distinct DNA copy number profiles of oncogenes and tumor

suppressor genes in chromosomal- and microsatellite-unstable sporadic colorectal carcinomas. *J Mol Med* 2007;85:293–304.
16. Tsafrir D, Bacolod M, Selvanayagam Z, Tsafrir I, Shia J, Zeng Z, Liu H, Krier C, Stengel RF, Barany F, Gerald WL, Paty PB, et al. Relationship of gene expression and chromosomal abnormalities in colorectal cancer. *Cancer Res* 2006;66:2129–37.
17. Sterian A, Kan T, Berki AT, Mori Y, Olaru A, Schulmann K, Sato F, Wang S, Paun B, Cai K, Hamilton JP, Abraham JM, et al. Mutational and LOH analyses of the chromosome 4q region in esophageal adenocarcinoma. *Oncology* 2006;70:168–72.
18. Takada H, Imoto I, Tsuda H, Sonoda I, Ichikura T, Mochizuki H, Okanoue T, Inazawa J. Screening of DNA copy-number aberrations in gastric cancer cell lines by array-based comparative genomic hybridization. *Cancer Sci* 2005;96:100–10.
19. Rajagopalan H, Jallepalli PV, Rago C, Velculescu VE, Kinzler KW, Vogelstein B, Lengauer C. Inactivation of hCDC4 can cause chromosomal instability. *Nature* 2004;428:77–81.
20. Kemp Z, Rowan A, Chambers W, Wortham N, Halford S, Sieber O, Mortensen N, von Herbay A, Gunther T, Ilyas M, Tomlinson I. CDC4 mutations occur in a subset of colorectal cancers but are not predicted to cause loss of function and are not associated with chromosomal instability. *Cancer Res* 2005;65:11361–6.
21. Welcker M, Singer J, Loeb KR, Grim J, Bloecher A, Gurien-West M, Clurman BE, Roberts JM. Multisite phosphorylation by Cdk2 and GSK3 controls cyclin E degradation. *Mol Cell* 2003;12:381–92.
22. Grandori C, Cowley SM, James LP, Eisenman RN. The Myc/Max/Mad network and the transcriptional control of cell behavior. *Annu Rev Cell Dev Biol* 2000;16:653–99.
23. Hwang HC, Clurman BE. Cyclin E in normal and neoplastic cell cycles. *Oncogene* 2005;24:2776–86.
24. Gu Z, Mitsui H, Inomata K, Honda M, Endo C, Sakurada A, Sato M, Okada Y, Kondo T, Horii A. The methylation status of FBXW7 beta-form correlates with histological subtype in human thymoma. *Biochem Biophys Res Commun* 2008;377:685–8.

WJGS World Journal of Gastrointestinal Surgery

Online Submissions: http://www.wjgnet.com/1948-9366office
wjgs@wjgnet.com
doi:10.4240/wjgs.v2.i3.89

World J Gastrointest Surg 2010 March 27; 2(3): 89-94
ISSN 1948-9366 (online)

CASE REPORT

Minute liver metastases from a rectal carcinoid: A case report and review

Hirofumi Yamamoto, Hideyuki Hemmi, Jin-Yu Gu, Mitsugu Sekimoto, Yuichiro Doki, Masaki Mori

Hirofumi Yamamoto, Hideyuki Hemmi, Mitsugu Sekimoto, Yuichiro Doki, Masaki Mori, Department of Surgery, Gastroenterological Surgery, Graduate School of Medicine, Osaka University; Osaka 565-0871, Japan

Jin-Yu Gu, the 3rd Department of General Surgery, the 2nd Affiliated Hospital of Harbin Medical University, Baojian Road 246, Nangang District, Harbin 150086, Heilongjiang Province, China

Author contributions: All authors contributed to this work; Yamamoto H wrote the manuscript; Hemmi H examined the past references; Gu JY performed the English editing; Sekimoto M performed the operation surgery; Doki Y and Mori M designed the study and revised the manuscript.

Correspondence to: Hirofumi Yamamoto, MD, PhD, Department of Surgery, Gastroenterological Surgery, Graduate School of Medicine, Osaka University, 2-2 Yamada-oka, Suita City, Osaka, 565-0871, Japan. hyamamoto@gesurg.med.osaka-u.ac.jp

Telephone: +81-6-68793251 Fax: +81-6-68793259

Received: August 12, 2009 Revised: September 7, 2009
Accepted: September 14, 2009
Published online: March 27, 2010

Abstract

We here report a 43-year-old male patient with minute liver metastases from a rectal carcinoid. Hepatic nodules were diagnosed during surgery, although they were not diagnosed by preoperative computed tomography or ultrasound examination. The rectal carcinoid was resected together with liver metastases and the patient has had no disease recurrence for 5 years following postoperative treatment of hepatic arterial infusion chemotherapy (HAIC) using 5-fluorouracil (5-FU) and oral administration of 1-hexylcarbamoyl-5-fluorouracil (HCFU). In 2003, a health check examination indicated presence of occult blood in his stool. Barium enema study revealed a rectal tumor in the lower rectum and colonoscopy showed a yellowish lesion with a size of 30 mm in diameter. Pathological examination of the biopsy specimen indicated that the rectal tumor was carcinoid. Although preoperative imaging examinations failed to detect liver metastases, 2 min nodules were found on the surface of liver during surgery. A rapid pathological examination revealed that they were metastatic tumors from the rectal carcinoid. Low anterior resection was performed for the rectal tumor and the pathological report indicated that there were 4 metastatic lymph nodes in the rectal mesentery. The patient received treatment by HAIC using 5-FU plus oral administration of HCFU and survived for 5 years. We also review world-wide current treatments and their efficacy for hepatic metastases of carcinoid tumors.

Key words: Hepatic arterial infusion chemotherapy; Rectal carcinoid; Liver metastasis; 5-Fluorouracil

Peer reviewer: Francis Seow-Choen, MBBS, FRCS, FAMS, Seow-Choen Colorectal Centre Pte Ltd, 3 Mt Elizabeth #09-10, Mt Elizabeth Medical Centre, Singapore

Yamamoto H, Hemmi H, Gu JY, Sekimoto M, Doki Y, Mori M. Minute liver metastases from a rectal carcinoid: A case report and review. *World J Gastrointest Surg* 2010; 2(3): 89-94 Available from: URL: http://www.wjgnet.com/1948-9366/full/v2/i3/89.htm DOI: http://dx.doi.org/10.4240/wjgs.v2.i3.89

INTRODUCTION

It is reported that the incidence of liver metastasis from gastrointestinal carcinoids is 16.7% (155 of 928) and the mean life span is approximately 2 years once liver metastasis is diagnosed[1-2]. With progress in treatments such as hepatic-artery embolization, radio-frequency thermal ablation, liver transplantation and others, the life span has been improved recently[3]. We report here a case of rectal carcinoid in a 43-year-old male with minute liver metastases that were diagnosed during surgery although preoperative computed tomography (CT) and ultrasonography (US) examination did not detect them. We employed hepatic

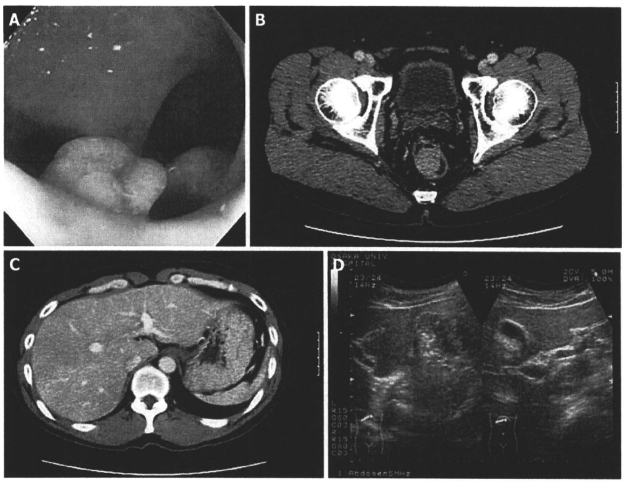

Figure 1 Preoperative colonoscopy and image examinations. A: Colonoscopy showed an elevated yellowish lesion with a slight central depression of which size was 30 mm in diameter, in the lower rectum; B: A tumor was present on the right wall of the lower rectum by computed tomography (CT) scan; C: Abdominal CT failed to show any obvious abnormalities in the liver; D: No obvious lesions were detected in the liver by ultrasonography.

Table 1 Blood test and urine 5-HIAA

WBC	6830/μL	AST	21 IU/L
RBC	$506x10^4$/μL	ALT	21 IU/L
Hb	15.4 g/dL	T.Bil	0.4 mg/dL
Ht	44.4%	T.P.	6.7 g/dL
Plt	$20.2x10^4$/μL	Alb	3.9 g/dL
		CRP	< 0.2 mg/dL
Na	140 mEq/L		
K	4.2 mEq/L	CA19-9	< 5.0 U/mL
Cl	107 mEq/L	CEA	1.0 ng/mL
BUN	14 mg/dL		
Cr	0.8 mg/dL	Urine 5-HIAA	1.3 mg/L

5-HIAA: 5-Hydroxy indole acetic acid.

arterial infusion chemotherapy (HAIC) using 5-fluorouracil (5-FU) and systemic administration of the oral 5-FU derivative 1-hexylcarbamoyl-5-fluorouracil (HCFU) as post-operative adjuvant therapy. The patient eventually survived 5 years after surgery without disease recurrence. Although the standard therapy for liver metastasis from carcinoid tumors has not been established in the world, several attractive strategies are currently provided, being reviewed together in this report.

CASE REPORT

A 43-year-old male patient entered our hospital in March 2003 because of a positive occult blood test on his stool samples. Through a barium enema study, a rectal tumor was suspected. He presented no carcinoid syndrome symptoms such as flushing, diarrhea, pellagra, cyanosis, and others. The results of blood test and level of 5-hydroxy indole acetic acid in the urine was within the normal range (Table 1).

Colonoscopy

Colonoscopy showed an elevated yellowish lesion in the lower rectum of 30 mm in diameter and with a slight central depression (Figure 1A). Pathological examination of biopsy samples revealed that this was a carcinoid tumor (data not shown).

Image examinations

CT scanning showed a tumor on the right wall of the lower rectum (Figure 1B). Abdominal CT failed to show any obvious abnormalities in the liver (Figure 1C). No obvious lesions were detected in the liver by abdominal US (Figure 1D).

Operation

During surgery, we perceived 2 min nodules through hand palpation of the surface of left liver lobe (S2 and S3). The nodules were hard and white and were both 2 mm in diameter. A rapid pathological examination revealed that the tumors were metastatic carcinoid (Figure 2A and 2B). Other hepatic abnormalities were not detected by intra-operative US. Low anterior resection of the rectum and partial resection of the liver (S2 and S3) were performed. The metastatic tumors were very small, indicating early phase metastases, and it was therefore likely that other latent metastases might be present in the liver. During surgery, we made preparation to carry our HAIC as a post-operative adjuvant chemotherapy, i.e. ligation of the right gastric artery and cholecystectomy to prevent the side effects such as gastric ulcer and cholecystitis, associated with HAIC.

Histopathological examination

Following staining of the primary rectal tumor with

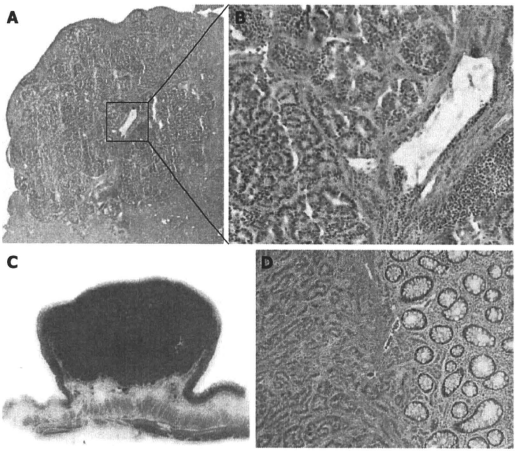

Figure 2 Histopathology of liver metastasis and primary tumor. A: Histopathology of a hepatic nodule (Magnification: × 20). A section was stained by hematoxiline & eosin (H&E) solution; B: Magnified image of (A) (Magnification: × 100): The tumor cells were homogeneous and spherical, forming ribbon-like structures, which was compatible with the carcinoid tumor; C: Resected rectal tumor. A loupe image; D: Histopathology of the rectal tumor (Magnification: × 100): Identical histopathological features to that of liver metastasis were confirmed.

Table 2 Hepatic resection for gastrointestinal carcinoid tumors

Author	*n*	5-year survival rate (%)	Ref.
Chamberlain *et al* (2000)	14	78	[14]
Nave *et al* (2001)	21	48	[15]
Norton *et al* (2003)	13	77	[16]
Sarmiento *et al* (2003)	120	62	[17]

Table 3 Liver transplantation for gastrointestinal carcinoid tumors

Author	*n*	5-year survival rate (%)	Ref.
Le Treut *et al* (1997)	15	69	[18]
Lehnert (1998)	36	50	[19]
Coppa *et al* (2001)	9	70	[20]

hematoxiline and eosin, histopathological examination showed homogeneous spherical cells, forming ribbon-like structures, compatible with the carcinoid tumor (Figure 2C and D). The tumor penetrated into the muscular propria without evidence of venous invasion or lymph duct invasion. There were 4 lymph node metastases within the rectal mesentery.

Post-operative adjuvant therapy

On the 35th day after surgery, a catheter was inserted from the left subclavian artery and the tip was set along common hepatic artery by the radiologists. HAIC using 5-FU started via the subcutaneous port. A dose of 1250 mg 5-FU was administered every week, and a total of 21 HAICs were performed. In addition, oral 5-FU, HCFU (Carmofur: 300 mg/d) was administered for one and half years as the lymph node metastases were positive. The patient was alive after 5 years without disease recurrence.

Table 4 Hepatic artery chemoembolization and hepatic artery embolization for metastatic carcinoid tumors

Author	%	Chemotherapy	Ref.
HACE			
Hajarizadeh *et al* (1992)	50.0 (4/8)	5-FU	[23]
Ruszniewski *et al* (1993)	33.3 (6/18)	DOX	[24]
Therasse *et al* (1993)	35.2 (6/17)	DOX	[25]
Kim *et al* (1999)	25.0 (4/16)	CDDP, DOX	[26]
Roche *et al* (2003)	42.8 (6/14)	DOX	[27]
	Total 35.6 (26/73)		
HAE			
Carrasco *et al* (1983)	83.3 (5/6)		[28]
Hanssen *et al* (1989)	71.4 (5/7)		[29]
Moertel *et al* (1994)	69.6 (16/23)		[30]
Wangberg *et al* (1996)	42.5 (17/40)		[31]
Eriksson *et al* (1998)	37.9 (11/29)		[32]
Loewe *et al* (2003)	72.7 (16/22)		[33]
	Total 55.1 (70/127)		

HACE: Hepatic arterial chemoembolization; HAE: Hepatic arterial embolization, CR: Complete response; PR: Partial response; CDDP: cisplatin; DOX: Doxorubicin; HAIC: Hepatic arterial infusion chemotherapy.

DISCUSSION

The 5-year survival rate of colorectal carcinoid is 72%-98%. However, once distant metastasis occurs the prognosis becomes poor[3-6]. In cases with liver metastasis, the 5-year survival rate is reported to be 19%-38%[7]. In Japan, most colorectal carcinoids are located in the rectum, mainly within 10 cm from the dentate line (80% of rectal carcinoids)[8]. Carcinoid tumors originate from the endocrine cells that produce certain amines and peptides. These cells are originally located in the deep mucosa. Once neoplastic changes occur, the tumor looks like a submucosal one following expansive growth.

Table 5 Reports of HAIC for hepatic metastasis of carcinoid tumor in Japan (1993 ~ 2006)

Age (yr)/ Gender	Agents 5FU	MMC	ADM	CDDP	MTX	VP16	FAR	Combined therapy	Effects	Ref.
69/M	o	o					o	-	PR	[35]
70/F	o			o				-	IR	[36]
42/M	o		o					-	PR	[37]
65/F	o				o			-	PR	[38]
56/M		o						5-FU	CR	[39]
52/M	o			o				DSM	PR	[40]
42/F	o							MTX + 5-FU	CR	[41]
3 cases	o	o						DSM	PR	[42]
68/M						o		-	PR	[43]
57/M	o	o		o				DSM	PR	[44]
49/F	o							-	CR	[45]

5-FU: 5-Fluorouracil; MMC: Mitomycin; ADM: Adriamycin; CDDP: Cisplatin; MTX: Methotrexate; VP16: Etoposide; FAR: Farmorubicin; DSM: Degradable starch microspheres; CR: Complete response; PR: Partial response; IR: Incomplete response.

With deeper invasion, the metastatic rate becomes correspondingly higher. The most frequent metastatic sites are lymph nodes and liver, followed by bone and lung. It is reported that the frequency of lymph node metastasis was 0% when the tumor is localized in mucosa, 5.3% in T1, 53% in T2 and 85.7% in T3[9]. Saito *et al*[10] also reported a relationship between tumor size and incidence of lymph node metastasis. When the tumor diameter is 6 to 10 mm, the metastasis rate is 0.7%, 11-15 mm: 23%, 16-20 mm: 55.6%, and > 21 mm: 66.7%.

There is a report that even 5mm-sized primary carcinoid tumor cause liver metastasis suggesting that a detailed examination of liver is essential before surgery[11]. US and CT scans are both standard modalities for detection of liver metastasis. Chiti *et al*[12] reported that the diagnostic sensitivity and specificity was 82% and 92%, respectively for US, and 73% and 93% for CT scans. In the case of the current patient with 2mm-sized liver metastatic lesions, preoperative abdominal US and CT failed to detect them, although such minute nodules could be easily perceived by hand palpation owing to their solidity. Therefore, intraoperative palpation of the liver surface is particularly important and should be done very carefully.

If the liver metastases are completely resected, surgery is the most effective therapy. The surgical indications include uni-lobar hepatic metastases, and multiple tumors expanding to both hepatic lobes with assurance of complete respectability based on good liver function. However, as approximately 90% of hepatic metastases are found to be multiple lesions in both hepatic lobes, complete resection is a rare event in practice[13]. The efficacy of hepatic resection for the gastrointestinal carcinoid tumors is summarized in Table 2[14-17].

Liver transplantation is an alternative treatment and widely adopted in patients with liver metastases from carcinoid tumors. The 5-year overall survival rate ranges from 50%-70% (Table 3)[18-20]. Lehnert[19] reported that the 5-year survival rate was 50% in 36 patients undergoing liver transplantation. He pointed out that the patients with extra-hepatic disease worsened the whole prognosis. Coppa *et al*[20] proposed that selection of patients with non-resectable metastastic neuroendocrine tumors for liver transplantation should be performed based on the Milan criteria: young patients < 50 years with confirmed by histology, with < 50% of the liver replaced by metastases, with a primary tumor (originating from the gastrointestinal tract) drained by the portal venous system, an absence of extrahepatic disease and stable disease during the pretransplantation period. They reported that the selected 9 cases who satisfied the criteria had a 70% 5-year overall survival rate and a 53% 5-year disease free survival rate.

Treatments by somatostatin analogues, such as interferon and octreotide have been reported. According to the findings, tumor shrinkage was a rare event although the systemic symptoms due to the carcinoid tumor were lessened[21-22].

Since liver metastases from carcinoids display an abundant tumor vascularity, hepatic arterial chemoembolization (HACE) or hepatic arterial embolization (HAE) are employed in western countries. The efficacy of HACE, in which doxorubicin is often used as a principal drug, is 25%-50% (Table 4, upper column)[23-27]. Partial response or complete response) cases were reported with HACE treatment. On the other hand, HAE was able to achieve the higher efficacy of 70%-80%, and appears to confer better therapeutic effects than HACE as a whole (Table 4, the lower column)[28-33].

In Japan, HAIC is often used[34]. As shown in Table 5[35-45], continuous 5-FU infusion accompanied by other chemotherapeutic drugs is the basic treatment scheme and conferred favorable effects. Based on these reports, we employed HAIC using 5-FU infusion for the current case. Recently, degradable starch microspheres (DSM) have also been used in combination with HAIC[40,42,44]. The antitumor efficacy when using DSM is attributed to transient obstruction of hepatic artery and subsequent blood reperfusion, which causes high local concentration of chemo-agents during the early phase and induces free radical oxygen as a late effect[46].

As well for primary hepatocellular carcinoma, radiofrequency ablation (RFA) therapy is also applicable to

liver matastatic lesions from carcinoid tumors. The most appropriate application is in cases where tumor size is less than 3 cm in diameter. Hellman *et al*[47] reported that RFA treatment was performed in a group of 21 patients with a total of 43 carcinoid metastatic liver nodules. Therapeutic efficacy was observed in 15 patients, including 4 cases who attained complete ablation.

REFERENCES

1 **Soga J**. Carcinoid tumors-an analysis of 1342 cases. *Geka* 1989; **12**: 1397-1409
2 **Soga J**, T Suzuki. Carcinoids and the carcinoid symdrome. *Nipponmishou* 1993; **51**: 207-221
3 **Modlin IM**, Sandor A. An analysis of 8305 cases of carcinoid tumors. *Cancer* 1997; **79**: 813-829
4 **Thompson GB**, van Heerden JA, Martin JK Jr, Schutt AJ, Ilstrup DM, Carney JA. Carcinoid tumors of the gastrointestinal tract: presentation, management, and prognosis. *Surgery* 1985; **98**: 1054-1063
5 **Modlin IM**, Lye KD, Kidd M. A 5-decade analysis of 13,715 carcinoid tumors. *Cancer* 2003; **97**: 934-959
6 **Crocetti E**, Paci E. Malignant carcinoids in the USA, SEER 1992-1999. An epidemiological study with 6830 cases. *Eur J Cancer Prev* 2003; **12**: 191-194
7 **Dawes L**, Schulte WJ, Condon RE. Carcinoid tumors. *Arch Surg* 1984; **119**: 375-378
8 **Iwashita A**, Hasegawa S, Haraoka S. Carcinoid tumors of the colon and rectum-including a standard for evaluating of curability of endoscopic resection. *Early Colorectal Cancer* 2002; **6**: 249-258
9 **Kotake K**, Yoneyama K, Miyata J. Carcinoid tumors of the rectum-Report of five cases a review of Japanese literature. *Daichoukoumongeka Gakkai Zasshi* 1984; **37**:261-266
10 **Saito Y**, Iwashita A, Iida M. A questionnaire survey concerning colorectal carcinoid tumors-Therapeutic strategy for colorectal carcinoid tumors. *Stomach and Intestine* 2005; **40**: 200-213
11 **Tsuboi K**, Shimura T, Suzuki H, Mochiki E, Haga N, Masuda N, Soda M, Yamamoto H, Asao T, Kuwano H. Liver metastasizes of a minute rectal carcinoid less than 5mm in diameter: A case report. *Hepatogastroenterology* 2004; **51**: 1330-1332
12 **Chiti A**, Fanti S, Savelli G, Romeo A, Bellanova B, Rodari M, van Graafeiland BJ, Monetti N, Bombardieri E. Comparison of somatostatin receptor imaging, computed tomography and ultrasound in the clinical management of neuroendocrine gastro-entero-pancreatic tumours. *Eur J Nucl Med* 1998; **25**: 1396-1403
13 **Ihse I**, Persson B, Tibblin S. Neuroendocrine metastases of the liver. *World J Surg* 1995; **19**: 76-82
14 **Chamberlain RS**, Canes D, Brown KT, Saltz L, Jarnagin W, Fong Y, Blumgart LH. Hepatic neuroendocrine metastases: does intervention alter outcomes? *J Am Coll Surg* 2000; **190**: 432-445
15 **Nave H**, Mössinger E, Feist H, Lang H, Raab H. Surgery as primary treatment in patients with liver metastases from carcinoid tumors: a retrospective, unicentric study over 13 years. *Surgery* 2001; **129**: 170-175
16 **Norton JA**, Warren RS, Kelly MG, Zuraek MB, Jensen RT. Aggressive surgery for metastatic liver neuroendocrine tumors. *Surgery* 2003; **134**: 1057-1063; discussion 1063-1065
17 **Sarmiento JM**, Heywood G, Rubin J, Ilstrup DM, Nagorney DM, Que FG. Surgical treatment of neuroendocrine metastases to the liver: a plea for resection to increase survival. *J Am Coll Surg* 2003; **197**: 29-37
18 **Le Treut YP**, Delpero JR, Dousset B, Cherqui D, Segol P, Mantion G, Hannoun L, Benhamou G, Launois B, Boillot O, Domergue J, Bismuth H. Results of liver transplantation in the treatment of metastatic neuroendocrine tumors. A 31-case French multicentric report. *Ann Surg* 1997; **225**: 355-364
19 **Lehnert T**. Liver transplantation for metastatic neuroendocrine carcinoma: an analysis of 103 patients. *Transplantation* 1998; **66**: 1307-1312
20 **Coppa J**, Pulvirenti A, Schiavo M, Romito R, Collini P, Di Bartolomeo M, Fabbri A, Regalia E, Mazzaferro V. Resection versus transplantation for liver metastases from neuroendocrine tumors. *Transpl Proc* 2001; **33**: 1537-1539
21 **di Bartolomeo M**, Bajetta E, Buzzoni R, Mariani L, Carnaghi C, Somma L, Zilembo N, di Leo A. Clinical efficacy of octreotide in the treatment of metastatic neuroendocrine tumors. A study by the Italian Trials in Medical Oncology Group. *Cancer* 1996; **77**: 402-408
22 **Bajetta E**, Zilembo N, Di Bartolomeo M, Di Leo A, Pilotti S, Bochicchio AM, Castellani R, Buzzoni R, Celio L, Dogliotti L. Treatment of metastatic carcinoids and other neuroendocrine tumors with recombinant interferon-alpha-2a. A study by the Italian Trials in Medical Oncology Group. *Cancer* 1993; **72**: 3099-3105
23 **Hajarizadeh H**, Ivancev K, Mueller CR, Fletcher WS, Woltering EA. Effective palliative treatment of metastatic carcinoid tumors with intra-arterial chemotherapy/chemoembolization combined with octreotide acetate. *Am J Surg* 1992; **163**: 479-483
24 **Ruszniewski P**, Rougier P, Roche A, Legmann P, Sibert A, Hochlaf S, Ychou M, Mignon M. Hepatic arterial chemoembolization in patients with liver metastases of endocrine tumors. A prospective phase II study in 24 patients. *Cancer* 1993; **71**: 2624-2630
25 **Therasse E**, Breittmayer F, Roche A, De Baere T, Indushekar S, Ducreux M, Lasser P, Elias D, Rougier P. Transcatheter chemoembolization of progressive carcinoid liver metastasis. *Radiology* 1993; **189**: 541-547
26 **Kim YH**, Ajani JA, Carrasco CH, Dumas P, Richli W, Lawrence D, Chuang V, Wallace S. Selective hepatic arterial chemoembolization for liver metastases in patients with carcinoid tumor or islet cell carcinoma. *Cancer Invest* 1999; **17**: 474-478
27 **Roche A**, Girish BV, de Baère T, Baudin E, Boige V, Elias D, Lasser P, Schlumberger M, Ducreux M. Trans-catheter arterial chemoembolization as first-line treatment for hepatic metastases from endocrine tumors. *Eur Radiol* 2003; **13**: 136-140
28 **Carrasco CH**, Chuang VP, Wallace S. Apudomas metastatic to the liver: treatment by hepatic artery embolization. *Radiology* 1983; **149**: 79-83
29 **Hanssen LE**, Schrumpf E, Kolbenstvedt AN, Tausjø J, Dolva LO. Recombinant alpha-2 interferon with or without hepatic artery embolization in the treatment of midgut carcinoid tumours. A preliminary report. *Acta Oncol* 1989; **28**: 439-443
30 **Moertel CG**, Johnson CM, McKusick MA, Martin JK Jr, Nagorney DM, Kvols LK, Rubin J, Kunselman S. The management of patients with advanced carcinoid tumors and islet cell carcinomas. *Ann Intern Med* 1994; **120**: 302-309
31 **Wängberg B**, Westberg G, Tylén U, Tisell L, Jansson S, Nilsson O, Johansson V, Scherstén T, Ahlman H. Survival of patients with disseminated midgut carcinoid tumors after aggressive tumor reduction. *World J Surg* 1996; **20**: 892-899; discussion 899
32 **Eriksson BK**, Larsson EG, Skogseid BM, Löfberg AM, Lörelius LE, Oberg KE. Liver embolizations of patients with malignant neuroendocrine gastrointestinal tumors. *Cancer* 1998; **83**: 2293-2301
33 **Loewe C**, Schindl M, Cejna M, Niederle B, Lammer J, Thurnher S. Permanent transarterial embolization of neuroendocrine metastases of the liver using cyanoacrylate and lipiodol: assessment of mid- and long-term results. *AJR Am J Roentgenol.* 2003; **180**: 1379-1384
34 **Hoshino H**, Ichikawa M, Onizuka. A case of rectal carcinoid with multiple hepatic metastases. *Daichoukoumongeka Gakkai Zasshi* 1991; **44**: 73-80
35 **Asai A**, Ando M, Kushida T. A case of metastatic liver tumors of the rectal carcinoid treated with hepatic artery ligation and catheterization. *Rinshogeka Gakkai Zasshi* 1993; **54**: 1862-1866

36 **Kirisu Y**, Kurayoshi K, Hoshino K. A case of carcinoid tumor of the rectum metastasizing to the liver and pancreas. *Shoikakigeka Gakkai Zassi* 1994; **27**: 1127-1131

37 **Hisamithu K**, Makino M, Kimura O. A case of carcinoid of rectum in which intrahepatic chemotherapy was effective for multiple liver metastases. *Rinshogeka Gakkai Zasshi* 1996; **57**: 918-921

38 **Takeuchi I**, Ishida H, Suzuki T. A case of liver metastases of restal carcinoid successfully treated with hepatic arterial infusion of methotrexate and 5-fluorouracil. *Jpn J Cancer Chemother* 1999; **26**: 1929-1932

39 **Nakagawa K**, Abe H, Momono S. A case of cecal carcinoid in which intrahepatic chemotherapy was effective for multiple liver metastases. *Daichoukoumongeka Gakkai Zasshi* 1999; **52**: 342-346

40 **Doi T**, Homma H, Mezawa S. A case of multiple liver metastases from rectal carcinoid tumor successfully treated with arterial infusion chemotherapy using degradable starch microspheres (DSM). *Shokakibyo Gakkai Zasshi* 2001; **98**: 410-415

41 **Sumi K**, Ataka M, Oka A. A case of rectal carcinoid tumor with hepatic and peritoneal metastases in which systemic CDDP+5FU and intrahepatic arterial infusion therapy with 5FU was successful. *Rinshogeka Gakkai Zasshi* 2001; **62**: 2489-2493

42 **Takanashi K**, Homma H, Mezawa S, Doi T, Akiyama T, Machida T, Murakami K, Hirata K, Iyama S. [Three cases of multiple liver metastases of carcinoid tumor responding to hepatic arterial infusion chemotherapy using degradable starch microspheres] *Gan To Kagaku Ryoho* 2002; **29**: 2358-2361

43 **Murase K**, Shimamoto T, Kondo T, Sugimoto T, Ozeki Y. [A long-term survival case of hepatic metastasis of rectal carcinoid in which etoposide was effective] *Nippon Shokakibyo Gakkai Zasshi* 2004; **101**: 47-51

44 **Shibutani Y**, Tani S, Uchikaga O. A case of multiple liver metastasis of rectal carcinoid tumor which occurred 10years after, responding to hepatic arterial infusion chemotherapy using Degradable Starch Microspheres. *Kounanbyouin Igaku Zassi* 2005; **22**: 1-4

45 **Nishimura A**, Hashizume T, Shibasaki I. Rectal carcinoid tumor with multiple liver metastases in which multidisciplinary therapy was successful-A case report-. *Rinshogeka Gakkai Zasshi* 2006; **67**: 679-682

46 **Yoshikawa T**, Kokura S, Oyamada H, Iinuma S, Nishimura S, Kaneko T, Naito Y, Kondo M. Anti tumor effect of ischemia-reperfusion injury induced by transient embolization. *Cancer Res* 1994; **54**: 5033-5035

47 **Hellman P**, Ladjevardi S, Skogseid B, Akerström G, Elvin A. Radiofrequency tissue ablation using cooled tip for liver metastases of endocrine tumors. *World J Surg* 2002; **26**: 1052-1056

S- Editor Li LF **L- Editor** Hughes D **E- Editor** Yang C

Journal of Surgical Oncology 2010;101:376–383

Multidetector Computed Tomography for Preoperative Prediction of Postsurgical Prognosis of Patients with Extrahepatic Biliary Cancer

SHOGO KOBAYASHI, MD, PhD,[1] HIROAKI NAGANO, MD, PhD,[1]* SHIGERU MARUBASHI, MD, PhD,[1] HIROSHI WADA, MD, PhD,[1] HIDETOSHI EGUCHI, MD, PhD,[1] YUTAKA TAKEDA, MD, PhD,[1] MASAHIRO TANEMURA, MD, PhD,[1] TONSOK KIM, MD, PhD,[2] YUICHIRO DOKI, MD, PhD,[1] AND MASAKI MORI, MD, PhD[1]

[1]*Department of Surgery, Osaka University, Yamadaoka 2-2(E2), Suita, Osaka, Japan*
[2]*Department of Surgery and Radiology, Osaka University, Yamadaoka 2-2(E2), Suita, Osaka, Japan*

Background: Preoperative prognostic information to select a treatment strategy is important especially in patients who need highly aggressive surgery, such as those with biliary cancer. We evaluated various prognostic factors and non-curative surgical factors using multidetector computed tomography (MDCT).

Methods: We retrospectively analyzed 71 patients who underwent MDCT preoperatively and were scheduled for surgical resection of biliary cancer. For MDCT diagnosis, we used MDCT-based classification equivalent to the surgical and pathological classification of the Japanese Society of Biliary Surgery. We evaluated MDCT-related prognostic factors and non-curative surgical factors and compared these factors with pathological results.

Results: MDCT-diagnosed category T (primary tumor invasion) included both prognostic factors and non-curative surgical factors but not category N (lymph node metastasis). Multivariate analysis identified MDCT-based suspected arterial invasion as an independent prognostic factor. In patients suspected of arterial invasion by MDCT, the 3-year overall survival rate was only 39% and the curative resection ratio was only 33%, because of the high positive surgical dissected margin.

Conclusion: MDCT-based suspected arterial invasion is a predictor of poor prognosis after surgery for biliary cancer and represents a non-curative surgical factor associated with positive dissected margin.
J. Surg. Oncol. 2010;101:376–383. © 2010 Wiley-Liss, Inc.

KEY WORDS: biliary cancer; surgery; MDCT

INTRODUCTION

At present, complete resection is one of the most effective treatments for local extrahepatic biliary cancer. The indication and selected type of surgery are based on the results of various imaging studies; however, the rate of curative resection according to the Japanese Society of Biliary Surgery (JSBS) has not exceeded 80% [1,2]. On the other hand, the development of multidetector computed tomography (MDCT) allowed establishing accurate diagnosis, especially in vertical extension [3], that is, invasion of the hepatic artery or portal vein. Okumoto et al. [4] reported the relationship between CT images of biliary tract tumors and histopathological invasion.

The resection procedure for biliary cancer is often aggressive. Therefore, understanding the preoperative factors that influence prognosis and curative resection might help in the selection of appropriate surgical strategy and avoid unnecessary surgery, which could ultimately improve prognosis. Based on the above reasons, we evaluated the prognostic factors in MDCT-based preoperative diagnosis in patients who were planned for curative resection. For the evaluation, we established criteria for MDCT-based diagnosis based on the surgical criteria of JSBS [1], which were also closely related to the CT-based diagnostic criteria recommended by Okumoto et al. [4]. This approach stemmed from the lack of appropriate criteria for MDCT-diagnosis that correlate with the surgical and pathological classifications. Analysis of preoperative MDCT data could provide a better prediction of prognosis, to select appropriate treatment, including surgery and neoadjuvant therapy.

Previous studies reported the relationship between diagnosis by MDCT and pathological diagnosis [4–13] in about 20 patients; however, there was no data for the respectability and/or the prognosis related to MDCT diagnosis. Recently, another strategy for biliary cancer, other than surgery, for example, chemotherapy with or without irradiation, has been tested. Information on the curative resection rate and prognosis of patients scheduled for surgery are important for any decision on treatment strategies. In the present study, we evaluated the prognostic and non-curative surgical factors among MDCT-related factors in cases planned for surgery.

Abbreviations: CEA, carcino-embryonic antigen; CTC, circulating tumor cells; fCur, final curability; FDG–PET, F-fluorodeoxyglucose–positron emission tomography; fStage, final stage; JSBS, Japanese Society of Biliary Surgery; MDCT, multidetector computed tomography; MRI, magnetic resonance imaging; OS, overall survival rate; PTPE, percutaneous transhepatic portal vein embolization; qPCR; quantitative polymerase chain reaction; SUV, standardized uptake values.

Contribution of Each Author: "designed research/study" Hiroaki Nagano, Yuichiro Doki, Masaki Mori, "performed research/study" Shogo Kobayashi, Shigeru Marubashi, "contributed important reagents" none, "collected data" Hidetoshi Eguchi, Yutaka Takeda, Masahiro Tanemura, "analyzed data" Shogo Kobayashi, "wrote the paper " Shogo Kobayashi, Hiroaki Nagano.

*Correspondence to: Hiroaki Nagano, MD, PhD, Department of Surgery, Graduate School of Medicine, Osaka University, Yamadaoka 2-2(E2), Suita, Osaka 565-0871, Japan. Fax: +81-6-6879-3259.
E-mail: hnagano@gesurg.med.osaka-u.ac.jp

Received 29 September 2009; Accepted 17 December 2009
DOI 10.1002/jso.21501
Published online 8 March 2010 in Wiley InterScience (www.interscience.wiley.com).

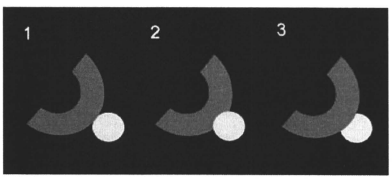

Fig. 1. Schematic diagram of MDCT-based diagnosis of invasion in biliary cancer. Gray open circle: biliary duct with cancer, white closed circle: enhanced vessels by contrast media. (1) Doubtful invasion: suspected cancer of the biliary duct attached to the vessel at a single point without space. (2) Definite invasion: suspected cancer of the biliary duct widely attached to the vessel; the latter shows no narrowing. (3) Severe invasion: suspected cancer of the biliary duct apparently invading the vessel and the vessel shows narrowing or obstruction.

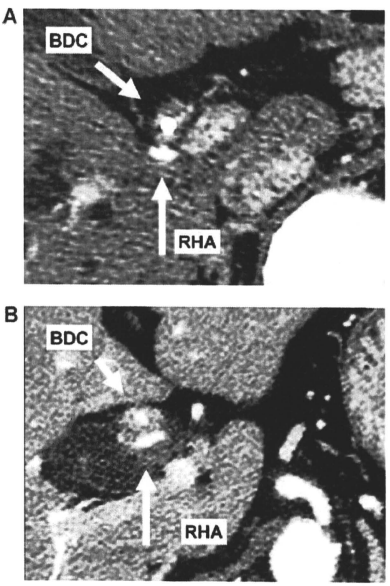

Fig. 2. Representative figure of CT-A. The figure showed the tumor (BDC) closely attached to the right hepatic artery (RHA). **A**: CT-A1, **B**: CT-A2.

PATIENTS AND METHODS

MDCT Criteria for Diagnosis and Rules for Classification of Cholangiocarcinoma

In this study, we used JSBS general rules for classification of biliary cancer: Surgical and Pathological Studies on Cancer of the Biliary Tract (5th edition) [1] to establish our criteria for MDCT diagnosis (Figure 1 and Table IA). These criteria were closely related to the CT diagnostic criteria of Okumoto et al. [4] for vascular invasion. The schematic diagram in the Figure 2 illustrates our classification of invasion and comparison with JSBS classification for surgery and pathology as well as the CT classification used by Okumoto et al. [4]. As example, we showed JSBS classification of extrahepatic bile duct cancer in Table IB.

Patients

We retrospectively analyzed all 71 patients who underwent MDCT preoperatively and who were scheduled for surgical resection up to 2007 at our institution. Table II shows the clinicopathological features of these patients. The median follow-up period was 18.4 months (range, 0.3–96.7), and during this follow-up period 27 (38.0%) patients died. All patients received regular follow-up with abdominal CT and measurement of serum carcinoembryonic antigen (CEA) every 3 months in the first 2 years and every 6 months later after

TABLE IA. Diagnostic Criteria for Preoperative MDCT, Based on JSBS Surgical Criteria

JSBS classification	Our MDCT criteria	CT criteria of Okumoto et al. [4]
Invasion of the hepatic artery (A) or portal vein (PV)		
0: No invasion		0
1: Doubtful invasion	Main tumor attached to the vessel	1a
2: Definite invasion	Between 1 and 3	1b, 2
3: Severe invasion (narrowing or obstruction)	Main tumor clearly invading the vessel	3, 4
Invasion of the liver (Hinf), biliary duct (Binf), and gall bladder (Ginf), pancreas (Panc)		
0: No invasion		
1: Doubtful invasion	Main tumor attached to the liver	
2: Definite invasion, but around the primary tumor	Main tumor clearly invading the liver	
3: Severe invasion but around the primary tumor	Main tumor severely invading the liver	
Invasion of the serosa		
0: No invasion		
1: Doubtful invasion	Main tumor attached to the serosa	
2: Definite invasion	Between 1 and 3	
3: Invasion of other organs	Main tumor invading other organs	
Lymph node metastasis		
0: No evidence of lymph node metastasis	Major axis <1 cm	
1: Lymph node metastasis	Major axis ≥ 1 cm	

TABLE IB. JSBS Classification in Extrahepatic Bile Duct Cancer

T category (pathological T category (pT)), primary tumor invasion					
(p)T1	S0 (m, fm)	(p)Hinf0	(p)Panc0	(p)PV0	(p)A0
(p)T2	S1 (ss)	Hinf1 (pHinf1a)	Panc1(pPanc1a)	(p)PV0	(p)A0
(p)T3	S2,3 (se)	Hinf1 (pHinf1b)	Panc1(pPanc1b)	(p)PV0	(p)A0
(p)T4	Any (any)	(p)Hinf 2,3	(p)Panc 2,3	(p)PV 1,2,3	(p)A 1,2,3

S, Hinf, Panc, PV, A were abbreviated at table 1A.

N category (lymph node metastasis groups)

N1: lymph node around the extrahepatic biliary duct.

N2: lymph node in the hepatoduodenal ligament, around common hepatic artery, and around superior retropancreas.

N3: the other lymph node around pancreas than N1 and N2, lymph node around celiac artery, and paraaortic lymph node.

Surgical stage (sStage) and final stage (fStage)

	H0, P0, M(-)				H1,2,3 P1,2,3, M(+)
	(p)N0	(p)N1	(p)N2	(p)N3	
(p)T1	I	II		IVa	IVb
(p)T2	II	III			
(p)T3			IVa		
(p)T4	IVa				

Final curability (fCur)

	H	P	pN·D	pDM	pHM	pEM	M
fCur A	H0	P0	pN<D	pDM0	pHM0	pEM0	M(-)
fCur B	Other than fCur A and fCur C						
fCur C	H1,2,3	P1,2,3	pN>D	pDM2	pHM2	pEM2	M(+)

H0 = no evidence of liver metastasis; H1 = metastasis limited to one lobe; H2 = a few metastases to both lobes; H3 = numerous metastases to both lobes; P0 = no evidence of peritoneal metastasis; P1 = metastasis to the peritoneum adjacent to extrahepatic bile ducts; P2 = a few metastases to the distant peritoneum; P3 = numerous metastases to the distant peritoneum; M = distant metastasis other than peritoneal and/or liver metastases; pN = histological lymph node metastasis; D = lymph node dissection; pDM = distal (duodenal) cut end; pHM = proximal (hepatic) cut end; pEM = dissected periductal structure; pDM0, pHM0, pEM0 = cancer-free margin of more than 5 mm in width; pDM1, pHM1, pEM1 = cancer-free margin of 5 mm or less in width; pDM2, pHM2, pEM2 = definite invasion of each surgical margin.

surgery. Eight (11.3%) received adjuvant therapy (five chemotherapy that included two on gemcitabine and three radiotherapy). Recurrence developed in 27 (38.0%) patients and 13 were treated with gemcitabine, while 2 received radiotherapy.

MDCT Imaging

MDCT was performed either with a LightSpeed Qxi scanner (GE Medical Systems, Waukesha, WI), a LightSpeed VCT scanner (GE Medical Systems) or with an Aquilion 64 scanner (Toshiba Medical Systems, Tokyo, Japan) using a tube voltage of 120 kV, a tube current of 300 mA, and a rotation time of 0.5 sec. Images of at least 0.625-mm slice thickness were used for evaluation. Contrast-enhanced multiphasic CT images were acquired at 10 sec after the peak aortic enhancement (arterial phase), followed by the portal venous phase and hepatic venous phase for the upper abdomen. Non-ionic contrast medium (300 mg/ml iodine) was administered intravenously at a rate of 2–4 ml/sec using a power injector.

CT-Based Staging

All CT images were used for staging. At least two radiologists or surgeons staged the disease preoperatively, according to the above classification, using preoperative MDCT. Trans-ampullary biliary drainage was performed in 22 (31.0%) patients during MDCT. We evaluated the invasion of the primary tumor into the hepatic artery (CT-A), portal vein (CT-PV), serosa (CT-S), and adjacent organs (liver, gall bladder from the bile duct, bile duct from the gall bladder,

TABLE II. Clinicopathological Features of Participating Patients and Their Survival Rate

	N	3-year overall survival rate (%)	P
Age (years)			
≥65	43	48	0.3541
<65	28	64	
Sex			
Male	43	48	0.3402
Female	28	67	
Diagnosis			
Extrahepatic bile duct	40	50	0.3885
Gall bladder	22	54	
Ampulla of Vater	9	76	
pT			
1/2/3	29	71	0.0009
4	29	35	
pN			
0/1	41	59	0.0853
2/3	24	42	
fStage			
1/2/3	23	78	0.0006
4a/b	35	6	
fCur			
A/B	49	63	0.0105
C	22	32	

and pancreas) and decided on the T category (CT-T) using JSBS classification for surgery. After evaluation of lymph node metastasis by MDCT (major axis ≥1 cm was considered positive, CT-N) we judged the CT-based stage (CT-stage).

Pathological Diagnosis

Pathological diagnosis was based on JSBS classification. For histopathological examination, 6-μm paraffin-embedded sections were prepared for each 5-mm serial section along the axial length of the biliary tract. The pathological diagnosis was compared retrospectively with CT-based diagnosis. For example, pathological invasion of the hepatic artery was abbreviated as pA, and pA1, pA2, pA3 indicated invasion of the adventitia, media, intima, and/or lumen of the hepatic artery, respectively.

Statistical Analysis

Overall survival (OS) rates were calculated by the Kaplan–Meier method and differences in CT-diagnosis factors were tested by the log-rank test. Differences in the curative resection ratio and the relationship between CT-N and pathological lymph node metastasis were analyzed by the Student's *t*-test or chi-square test. Multivariate analysis was performed using Cox proportional-hazards regression model. A P value of <0.05 was considered statistically significant. The statistical software used was StatView J-5.0 software (SAS, Cary, NC).

RESULTS

Patients Survival Rate According to Pathological Diagnosis

Table II also shows patients survival according to pathological diagnosis. The OS rate at 3 years was 54.3%. The curative resection ratio (fCurA and B) was 69%. The pathological prognostic factors were T category (pT), final stage (fStage), and final curability (fCur) similar to other patients with biliary cancer, except for a trend in pathological lymph node metastasis (pN, $P = 0.0853$).

Overall Survival Rate According to MDCT-Based Diagnosis

Based on the above classification for preoperative MDCT-diagnosis, CT-staging was performed and the CT-stage-dependent survival was calculated (Table III). There was a significant difference

TABLE III. MDCT Staging and Prognosis

	n	3-year overall survival rate (%)	Univariate P	Multivariate Hazard ratio	Multivariate 95% CI	Multivariate P
CT-T						
T1/2/3	33	75	0.0050			
T4	38	36				
CT-N						
N0/1	48	63	0.6052			
N2/3	23	43				
CT-Stage						
Stage 1/2	26	79	0.0649			
Stage 3/4a	30	51				
Stage 4b	15	26				
CT-A						
A0	41	67	0.0163	2.625	1.176–5.848	0.0184
A1/2/3	30	39				
CT-PV						
PV0	51	56	0.4082			
PV1/2/3	20	51				
CT-S						
S0	10	62	0.2350			
S1	29	49				
S2/3	10	23				
CT-Hinf/Ginf/Binf/Panc						
0	47	62	0.0492	2.077	0.966–4.467	0.0614
1	9	56				
2/3	15	28				

TABLE IV. MDCT Staging Rate for fCurA/B Resection

	n	fCurA/B	Rate (%)	P
CT-T				
1/2/3	33	28	85	0.0072
4	38	21	55	
CT-N				
0	44	33	75	0.2701
1	4	2	50	
2	16	9	56	
CT-Stage				
1/2	26	22	85	<0.0001
3/4a	30	20	67	
4b	8	0	0	
CT-A				
0	41	35	85	0.0017
1	24	12	50	
2/3	6	2	33	
CT-P				
0	51	39	76	0.0836
1	13	6	46	
2/3	7	4	57	
CT-S				
0	10	9	90	0.0594
1	29	16	55	
2/3	10	4	40	
CT-Hinf/Ginf/Binf/Panc				
0	47	34	72	0.6583
1	9	6	67	
2/3	15	9	60	

in OS rate between CT-T 1/2/3 and CT-T 4 (3-year OS rates: 75% and 36%, respectively, $P = 0.0050$). However, there was no significant difference in OS rate based on CT-N. For category T, CT-A and invasion of adjacent organs correlated with prognosis, and multivariate analysis identified CT-A as the only independent factor related to prognosis (hazard ratio = 2.625, $P = 0.184$). The 3-year OS rate of patient with CT-A (CT-A 1/2/3) was 39%.

Curative Resection Rate in MDCT-Based Diagnosis

We also calculated the curative resection rate (rate of fCur A and B in JSBS classification) (Table IV). fCur A or B is defined as pathologically negative margin and wider lymph node dissection than pathological metastasis; in other words, R0 resection. CT-T correlated significantly with the curative resection ratio ($P = 0.0072$). The curative resection rate for CT-T4 was only 55%. For category T, curative resection correlated with only CT-A, and the curative resection rate for CT-A 2/3 was 33% ($P = 0.0017$).

We also analyzed the reasons for non-curative resection (fCur C, Table V). The major reason for non-curative resection in patients with CT-A0 was lymph node metastasis. In contrast, approximately 70% of patients with CT-A 1/2/3 have pathologically positive surgical margin and 45% of these patients had a positively dissected margin (Table V).

Relationship Between MDCT-Based Diagnosis and Pathological Diagnosis

We compared the relationship between MDCT-based diagnosis and pathological diagnosis based on JSBS classification for histopathological findings. To estimate lymph node metastasis (N category), we used the lymph node metastasis groups (Table VI). Twenty-four of 65 (37%) were diagnosed as CT-N-positive, while 31 (48%) were pathologically positive. However, there was no relationship between CT-N and pathological N (pathological lymph node metastasis, $P = 0.6631$, Table VI).

On the other hand, in T category, we compared CT-A factor (hepatic artery invasion), which correlated with OS and the curative resection ratio, with pathological diagnosis (pA, Tables VII and VIII). For factor A calculated for the whole biliary cancer (bile duct, gall bladder, and ampulla cancer), CT-A was positive (CT-A 1/2/3) in 12 patients among 41 fCur A/B patients (29%), whereas pathological A (pA) was positive in only a single CT-A1 patient. One patient classified as CT-A3 (ipsilateral artery of the resected liver) had no pathological invasion of the hepatic artery. On the other hand, in fCur C patients, 13 of 16 patients (81%) were CT-A positive (CT-A1/2/3), and 2 of these patients were classified pathologically to have arterial invasion (pA2). Three of these patients were CT-A2 or CT-A3 of ipsilateral artery of the resected liver; however, they were negative for pathological arterial invasion.

Furthermore, for hilar biliary cancer, hepatic artery invasion was more closely related to curative resection. We also analyzed the correlation between liver resection with contralateral hepatic artery resection and pathological diagnosis (Table VIII). The contralateral hepatic artery resection was performed in two patients and their pathological diagnosis for contralateral hepatic artery invasion was negative. Invasion of the hepatic artery was diagnosed pathologically in two of CT-A1 patients and these were ipsilateral hepatic artery of the resected liver. The pathological positive rate was 11% (2/18).

DISCUSSION

In this study, we evaluated MDCT-based prognostic factors using surgical and pathological classification-related criteria. For discussion of MDCT diagnosis, one should separately evaluate the three different components of tumor factors in biliary cancer: vertical extension (T category), horizontal extension, and lymph node metastasis (N category). We herein discuss CT-staging related factors: T and N category, excluding horizontal extension.

For the T category, CT-A 1/2/3 was both a prognostic factor and non-curative surgical factor. This factor did not correlate with pathological arterial invasion but was dissected margin-positive. Previous studies have not provided clear definition criteria for CT diagnosis of vascular invasion. Only Okumoto et al. [4] reported the relationship between MDCT and pathological diagnosis, and their criteria 1b (our CT-A2/3) correlated with pathological invasion of the right hepatic artery. In our study, only six cases were classified as CT-A2 (Okumoto's 1b) and the data on these patients could not define a clear relationship with the pathological diagnosis. On the other hand, 24 cases were diagnosed as CT-A1 and histopathological examination

TABLE V. Reasons for fCurC in MDCT-A Status

CT-A	n	fCurC (%)	Margin (+)[a]	Dissected margin (+)[b]
0	41	6 (15%)	0/6 (0%)	—
1/2/3	30	16 (53%)	11/16 (69%)	5/11 (45%)

[a]Pathologically positive surgical margin at hepatic, duodenal, or dissected periductal structures.
[b]Pathologically positive surgical margin at dissected periductal structures at least.